Pleiotropic function of ezrin in human metastatic melanomas

ARTICLE *in* INTERNATIONAL JOURNAL OF CANCER · JUNE 2009

Impact Factor: 5.09 · DOI: 10.1002/ijc.24255 · Source: PubMed

14 AUTHORS, INCLUDING:

Francesco Lozupone
Istituto Superiore di Sanità
35 PUBLICATIONS **1,943** CITATIONS
SEE PROFILE

Paola Matarrese
Istituto Superiore di Sanità
138 PUBLICATIONS **5,921** CITATIONS
SEE PROFILE

Serena Cecchetti
Istituto Superiore di Sanità
38 PUBLICATIONS **532** CITATIONS
SEE PROFILE

Walter Malorni
Istituto Superiore di Sanità
399 PUBLICATIONS **15,541** CITATIONS
SEE PROFILE

Int. J. Cancer: **124,** 2804–2812 (2009)

Pleiotropic function of ezrin in human metastatic melanomas

Cristina Federici[1], Daria Brambilla[1], Francesco Lozupone[1], Paola Matarrese[1], Angelo de Milito[1], Luana Lugini[2], Elisabetta Iessi[1], Serena Cecchetti[2], Marialucia Marino[1], Maurizio Perdicchio[1], Mariantonia Logozzi[1], Massimo Spada[2], Walter Malorni[1] and Stefano Fais[1]*

[1]*Department of Therapeutic Research and Medicines Evaluation, Istituto Superiore di Sanità, Rome, Italy*
[2]*Department of Cell Biology and Neurosciences, Istituto Superiore di Sanità, Rome, Italy*

The membrane cytoskeleton cross-linker, ezrin, has recently been depicted as a key regulator in the progression and metastasis of several pediatric tumors. Less defined appears the role of ezrin in human adult tumors, especially melanoma. We therefore addressed ezrin involvement in the metastatic phenotype of human adult metastatic melanoma cells. Our results show that cells resected from melanoma metastatic lesions of patients, display marked metastatic spreading capacity in SCID mice organs. Stable transfection of human melanoma cells with an ezrin deletion mutant comprising only 146 N-terminal aminoacids led to the abolishment of metastatic dissemination. *In vitro* experiments revealed ezrin direct molecular interactions with molecules related to metastatic functions such as CD44, merlin and Lamp-1, consistent with its participation to the formation of phagocitic vacuoles, vesicular sorting and migration capacities of melanoma cells. Moreover, the ezrin fragment capable of binding to CD44 was shorter than that previously reported, and transfection with the ezrin deletion mutant abrogated plasma membrane Lamp-1 recruitment. This study highlights key involvement of ezrin in a complex machinery, which allows metastatic cancer cells to migrate, invade and survive in very unfavorable conditions. Our *in vivo* and *in vitro* data reveal that ezrin is the hub of the metastatic behavior also in human adult tumors.

Key words: CD44; merlin; Lamp-1; phagocytic vacuole; organelle acidity

The molecular events governing progression from a primary tumor to an invasive, malignant tumor remain poorly defined despite intense scientific endeavor mostly due to molecular biology and biochemical data collected from non human models.[1]

The metastatic phenomenon is characterized by a cascade of events that assumes the existence of very harmful cells within the primitive tumor mass. These cells must acquire the ability to breach underlying basement membrane, migrate through interstitial stroma, gain access to and migrate through blood or lymphatic vessels, attach, enter, survive and proliferate within metastatic organs.

Mounting evidence suggesting that ezrin contributes to tumor metastasis promotion, arose mainly from experiments employing syngeneic implantation models correlated to gene expression profiling performed on pediatric tumors.[1,2] In human tumors, ezrin deregulation or impaired functionality is related to poor prognosis.[3–9]

Ezrin belongs to the MERM family of cytoskeleton-associated proteins[10] and functions as a linker between the actin cortical cytoskeleton and various membrane-bound molecules[11,12] through its C-terminal and N-terminal domains, respectively.

ERM proteins are implicated in a wide variety of important cellular processes.[10,13–18] Notably, ezrin is primarily involved in both cell-to-cell adhesion and cell adhesion to the ECM through association with ICAMs, CD44, E-cadherin and β-catenin.[12,19] To this family belongs also the tumor suppressor merlin (NF-2, schwannomin), whose loss is related to the development of tumors[20,21] and metastasis formation.[22]

Recently, we reported ezrin involvement in a mostly neglected tumor function such as phagocytic activity or cannibalism of metastatic melanoma cells, that is an exclusive property of cells derived from metastatic lesions.[23,24] However, we did not identify the specific ezrin interaction with cannibal vacuoles. Another footprint of malignancy is also represented by the localization on the cell plasma membrane of Lamp-1.[25] A possible explanation for this aberrant localization of an internal vacuole molecule might be the involvement with some peculiar functions of metastatic cells, such as Lamp-1/E-selectin interaction in tumor-endothelial cell adhesion.[26] Lamp-1 is a human phago-lysosome-associated membrane protein[27,28] whose expression is increased in metastatic tumor cells of various origins.[29–32]

Lamp-1 (also known as CD107a) is a heavily glycosylated, type I transmembrane protein that constitutes one of the two major sialoglycoproteins on lysosomal membranes. It is a widely expressed intracellular antigen ubiquitously expressed. Under physiological conditions, this lysosomal antigen functions in protecting the inner surface of the lysosomal membrane by forming a barrier to lysosomal hydrolases.[29]

Lamp-1 is also involved in adhesion of cancer cells to the ECM[25] and carries poly-N-acetyllactosamines,[33] in turn correlating with tumor metastatic potential.[30] This may be related to E-selectin-mediated increase in the adhesion of tumor cells to endothelial cells at metastatic sites.[26,29,34–36]

In this study, we wanted to correlate ezrin molecular interactions with some major actors of the metastatic behavior of tumor cells (*i.e.*, CD44, Lamp-1 and merlin) to the *in vivo* dissemination of human malignant melanoma cells. To this purpose, we investigated growth and metastatic spreading of untransfected or stably transfected human melanoma cells with the ezrin deletion mutant ez-146. Moreover, we related the metastatic behavior with some metastasis-related functions, such as: migrating capacity, phagocytic activity and vesicular sorting, and reciprocal interaction of ezrin with molecules involved in these functions.

The results showed that ezrin exerts multiple roles in determining metastatic onset in human melanoma cells.

We newly show that ezrin's molecular interactions with proteins critical in conferring tumor cell metastatic potential, contributes not only to the ability of cells to migrate within tissues and through the body, but also survive and proliferate in condition of nutrients deprivation.

Material and methods

Animals and cell cultures

CB.17 SCID/SCID female mice (Charles River Laboratories, Italy) employed were of reproductive age (4–5 weeks old) and

Abbreviations: CD, cluster of differentiation; DMSO, Dimethyl sulfoxide; ECM, extracellular matrix; ERM, ezrin, radixin, moesin; ez-146, ezrin deletion mutant; ICAMs, intercellular adhesion molecules; Lamp-1, lysosomal-membrane-associated glycoprotein-1; MERM, merlin, ezrin, radixin, moesin; MM1-MM3, human metastatic melanoma cells; NERMAD, NH2-terminal ERM-associated domain; RT, room temperature.

The first two authors contributed equally to this work.
Grant sponsors: Ministero della Salute-Istituto San Gallicano.
***Correspondence to:** Department of Therapeutic Research and Medicines Evaluation, Istituto Superiore di Sanità, Viale Regina Elena 299, Rome, Italy. E-mail: stefano.fais@iss.it
Received 12 September 2008; Accepted after revision 18 December 2008
DOI 10.1002/ijc.24255
Published online 12 January 2009 in Wiley InterScience (www.interscience.wiley.com).

housed under specific pathogen free conditions, in microisolator cages. All experiments performed *in vivo* were carried out 3 times independently. Both the experiments and the animal care procedures conformed to current NIH guidelines.

Human melanoma cell lines used were the MM1, MM2 and MM3 obtained from melanomas of patients surgically resected at the Istituto di Tumori, Milan. These cell lines were derived from histologically diagnosed secondary melanoma lesions as previously described.[37]

HeLa cells were obtained from American Type Culture Collection (Manassas, VA). All cells were cultured in RPMI 1640 (GIBCO-Invitrogen, Milan, Italy) supplemented with 100 IU/mL penicillin, 100 μg/mL streptomycin (GIBCO) and 2 mmol/L glutamine (Life Technologies, Milan, Italy) with 10% FCS in a humidified incubator (37°C, 5% CO_2).

Chemicals

Bafilomycin A1 (Sigma-Aldrich, St. Louis, MO) was resuspended in DMSO and used at the indicated concentrations.

Engraftment and growth of human tumors in SCID mice and metastasis evaluation

Mice were injected s.c. into the right flank with 2×10^6 human melanoma cellular suspension/mouse. Tumor growth was monitored by measuring maximal and minimal diameters by calliper 3 times a week and tumor weight was estimated with the formula : tumor weight (mg)= [length (mm) $\times$ width^2 (mm)]/2, as previously described.[38]

After 45 days, mice were killed and the following organs: local lymph nodes, liver, and lungs were observed under a dissecting stereomicroscope for the presence of metastasis.

Tumor number was obtained by visual inspection of tissues. Detection of microscopic metastatic lesions was obtained by histological examination of paraffin sections.

Analysis of cell migration and invasion

Transwell migration assays were performed using 8-μm transwell inserts (BD, Franklin Lakes, NJ) suspended by the outer rim within individual wells of 6-well plates. In brief, cells (2×10^4 per well) were resuspended in RPMI supplemented with 5% FBS and plated in the upper chamber. The lower chamber was filled with RPMI supplemented with 10% FBS. Cells were allowed to migrate for 48 hr. Non migrated cells were removed from the upper chamber with a cotton swab and cells that had migrated and attached to the lower side of the filter were stained with Diff-Quik kit (BD bioscience) and enumerated using an ocular micrometer. A minimum of 10 random fields per filter were counted. Mean of migrated cells and their SD were calculated. All of the experiments were performed independently and in triplicate. GFP expression in transfected cells was evaluated by FACS analysis.

Invasion assay was performed employing (BD) BioCoat™ Matrigel™ Invasion Chambers according to manufacturer's instructions. After incubation at 37°C in a 5% CO2 atmosphere for 24 hr. Non invading cells were removed following the same procedure as that applied for the migration assay. Matrigel invading cells were fixed with 4% paraformaldehyde for 10 minutes and stained with 0.1% crystal violet for 15 minutes, then counted using a light microscope. The experiment was performed in triplicate.

Growth curves

Cell proliferation was analyzed by performing growth curves both in control and ez-146 transfected cells. Viability was evaluated employing the trypan blue exclusion test.

Transfection of melanoma cells

Primers utilized to direct synthesis of the GFP-full length wild-type ezrin (ezrin-GFP) fusion protein were 5′ CTGCAGACTCACC AGAAACCGA-3′ and 5′-GAATTCCAGGGCCTCGAACTCG-3′. PCR products were cloned into pTopo vector (GIBCO, Invitrogen) and then excised with the appropriate couple of restriction enzymes (XhoI-EcoRI) and ligated in the pEGFPN1 vector (Clontech Laboratories, Mountain View, CA) at the XhoI and EcoRI sites to produce the ezrin GFP fusion protein. The GFP-tagged deletion mutant 146 ezrin (ez-146) was obtained as a GFP-mutant ezrin fusion protein in which aminoacids 147–585 were deleted. Primers used were the following: 5′-CTGCAGACTCACCA GAAACCGA-3′ and 5′-GGTACCCAGACTTGTGCACTTC-3′. PCR product was cloned into pTopo vector (GIBCO, Invitrogen), then excised with *Xho*I and *Eco*RI restriction enzymes (Promega, Milan, Italy) and ligated in the pEGFP-N1 vector to produce the fusion protein. Plasmids encoding the GFP-fusion proteins were transfected either stably or transiently, as specified in the text, into melanoma cells (MM1-MM3) using Lipofectamine 2000 reagent (GIBCO-Invitrogen), following the manufacturer's protocol. Stably ez-146 GFP expressing cells were obtained after selection with gentamicin G.418 (Invitrogen).

Percentage of transfected cells was evaluated by FACS analysis. No alterations in terms of morphological features, proliferation and cell cycle progression were observed among the ez-146 GFP transfected clones as compared to ezrin-GFP transfected cells and untransfected cells.

Protein cross-linking, immunoprecipitation and Western blot

Cells were harvested at subconfluence and washed with PBS. Subsequently, protein cross-linking was performed by incubating each cell pellet in 0.5% paraformaldheyde solution for 60 minutes at room temperature (RT). The reaction was quenched with 1.25 mM glycine and incubated 5 minutes at RT. Preliminary results showed that the ability of our antibody to immunoprecipitate cross-linked ezrin was not influenced by the following panel of cross-linking methods evaluated: paraformaldehyde, ethylene glycol bis (succinimidyl succinate) (EGS) or dithio bis (succinimidyl propionate) (DSP).

After cross-linking, in the indicated experiments, proteins were subjected to immunoprecipitation and Western blot. In brief, subconfluent melanoma cells were either: lysed in AKT buffer [20 mmol/L Tris-HCl (pH 7.5), 150 mmol/L NaCl, 10% glycerol, 1% NP40] with protease inhibitors (10 μg/mL aprotinin and 2 mmol/L phenylmethylsulfonyl fluoride), subjected to cellular fractionation following the manufacturer's instruction of the Quiagen cell compartment kit (Quiagen, Germany) or were subjected to differential ultracentrifugation as described previously[39] to obtain a pellet enriched in endolysosomes.

Endolysosomal pellet was resuspended in immunoprecipitation buffer: 50 mmol/L HEPES (pH 6.9), 10 mmol/L EDTA, 1% Triton X-100, 300 mmol/L NaCl. Proteins were precleared with protein A/G-Sepharose 4B Fast Flow (Sigma-Aldrich).

For Ezrin and GFP-ez-146 were respectively immunoprecipitated from 1 mg precleared lysates with 3 μg anti-ezrin, clone 3C12 (Sigma-Aldrich) and 3 μg anti-GFP, clone 1E4 (MBL, Woburn, MA) Abs in the presence of protein A/G-Sepharose. Thirty microgram per sample were resolved on 8–12% acrylamide gel and transferred to nitrocellulose membrane Protran BA85 (Schleicher & Schuell, Keene, NH). Membranes were blocked overnight with 5% dry milk in PBS. Blotting was performed employing monoclonal antibody to Lamp-1 clone H4A3 (BD-Biosciences), ezrin (Sigma-Aldrich), and actin clone 10A5 (Chemicon International, CA). After incubation with appropriate peroxidase-conjugated anti IgG (Amersham Biosciences, Milan, Italy), membranes were revealed by enhanced chemiluminescence (Pierce, Rockford, IL). Membrane stripping was performed using Restore Western blot stripping buffer (Pierce), according to the manufacturer's instructions. Antibodies employed in Western blot, other than those mentioned: anti-HCAM clone F-4 (Santa Cruz Biotechnology, CA), anti-merlin clone A-19 (Santa Cruz), anti-GFP (MBL) Abs.

For depletion of wild type ezrin from ez-146 MM1, total cell extracts were subjected to immunoprecipitation with antibody

recognizing wild type ezrin employing a higher amount of the latter. Thirty microgram of supernatants of immunodepleted wild-type ezrin were used as negative controls and then employed for classical immunoprecipitation as described above.

Flow cytometry

For Lamp-1 surface detection, living cells were stained with a specific anti Lamp-1 Ab and then with an anti-mouse IgG PerCP/CY5.5-conjugated (Becton Dickinson). For total amount of Lamp-1 detection, immunostaining with the same antibody was performed in cells fixed with 4% paraformaldehyde and permeabilized with 0.05% Triton X-100 (Sigma). After immunostaining, samples were immediately analyzed on a FACScan or FACScalibur cytometer (BD Biosciences, Heidelberg, Germany). Surface Lamp-1 expression was described as percentage of positive cells, whereas total amount of Lamp-1 was expressed as median fluorescence intensity (MFI).

Flow cytometric fluorescence resonance energy transfer analysis

We applied fluorescence resonance energy transfer (FRET) analysis to demonstrate colocalization of ezrin and Lamp-1 in MM1–MM3. Briefly, cells were fixed and permeabilized using 2% paraformaldehyde for 24 hr and 0.05% Triton X-100 for 10 minutes at 4°C, respectively. After 2 washings in cold PBS the cells were labeled with mAbs tagged with donor (PE) or acceptor (Cy5) dyes. Ezrin staining was performed using unlabeled mouse anti-ezrin Ab clone 18 (Transduction Laboratories) and a saturating amount of Cy5 labeled anti-mouse IgG (BD Pharmingen, CA).

Lamp-1 was detected by anti-Lamp-1 Ab followed by biotinylated anti-rabbit IgG and then saturating concentrations of streptavidin-Cy5 (both from BD Pharmingen). Cells were analyzed with a dual-laser FACSCalibur. For determination of FRET efficiency, changes in fluorescence intensity of donor plus acceptor labeled cells were compared with the emission signal from cells labeled with donor-only and acceptor only fluorophores. All data were corrected for background by subtracting the binding of the isotype controls. Efficient energy transfer resulted in an increased acceptor emission on cells stained with both donor and acceptor dyes. The FRET efficiency (ET) was calculated according to[40] using the formula: ET=(FL3DA-FL2DA/a-FL4DA/b)/FL3DA, where A is the acceptor and D is donor, a = FL2D/FL3D and b = FL4A/FL3A.

Fluorescent microscopy

MM1 cells and GFP-ez-146 transfected counterpart were fixed and permeabilized as previously reported.[23] Samples were incubated at 37°C for 1hr with anti ezrin clone C-15 (Santa Cruz) and anti-Lamp-1 (BD Biosciences) Abs. After washings, cells were labeled with Alexa Fluor 488-conjugated anti-rabbit (Molecular Probes, Eugene, OR) plus Alexa Fluor 594-conjugated anti-mouse IgG (Molecular Probes). After washings, the samples were mounted with glycerol:PBS (1:1).

For acidic vesicle evaluation: LysoTracker Red DND-99 (1,000×; Invitrogen) accumulates in lysosomes and is employed for staining and semiquantitative evaluation of acidic intracellular organelles by fluorescence mycroscopy.[41] The probe was added to 2×10^5 fresh cells plated on cover slips either treated or not with bafilomycin A1 (5 nM for 2 hr) and incubated at RT for 30 minutes. Cells were then fixed with paraformaldehyde and stained with Hoechst 33245 (GIBCO, Invitrogen) to allow nuclear staining. The experiments were repeated at least thrice in duplicate wells, and untreated and unstained cells were used to set the background fluorescence.

All samples were observed with a Nikon Microphot fluorescence microscope. Images were captured by a color chilled 3CCD camera (Hamamatsu, Japan) and analyzed by the OPTILAB (Graftek, France) software.

Data analysis and statistical evaluation

For flow cytometry studies all samples were analyzed with a FACScan or FACScalibur cytometer (BD Biosciences, Heidelberg, Germany). At least 20,000 events were acquired. Data were recorded and statistically analyzed by a Macintosh computer using CellQuest Software. The total amount of Lamp-1 was expressed as median fluorescence and the statistical significance was calculated using the non-parametric Kolmogorov-Smirnov (K/S) test. The surface expression of Lamp-1 was indicated as percentage of positive cells and statistic analysis was performed using ANOVA two-way test for repeated samples using Graphpad software. All data reported in this article were verified in at least 3 independent experiments and reported as mean ± SD. For all the other experiments, differences between data were analyzed employing the Student's t test and as for flow cytometry studies, the statistically significant differences were defined only when $p < 0.01$.

Results

Over-expression of ez-146 inhibits metastasis of melanoma cells in vivo *without altering primary tumor growth*

To evaluate the involvement of ezrin in metastatic occurrence, we examined *in vivo* the effects of both constitutive and deletion mutant ezrin on invasion and dissemination of human melanoma cells deriving from metastatic lesions. Experiments were performed in a human tumor/SCID mice xenograft model (15), inoculated with either untransfected, ez-146 or full length ezrin-GFP transfected cells (MM1-MM3 and HeLa).

Prior to mice s.c. inoculation, ez-146 cells were compared with the untransfected counterpart and were indistinguishable *in vitro* from their wild-type untransfected as far as proliferation, growth and morphological features were concerned (data not shown). Up to 93.7% of the ez-146 cells were GFP positive.

The size of s.c. tumors were measured weekly during the engraftment period and after 6 weeks mice were killed and the various organs analyzed for the presence of metastatic lesions. Moreover, measurements of tumor growth did not show any difference between tumors developed in SCID mice inoculated with ez-146, ezrin-GFP transfected cells and untransfected counterpart (Table I). These data indicated that in the proposed model, ezrin was not involved in the growth of the primary tumor thus supporting previous reports.[1,3]

The presence of metastases in local lymph nodes, liver, and lungs was evaluated under a dissecting stereomicroscope. The results showed that 100% (10/10) of SCID mice with MM1 tumors developed lung and lymph node metastases, whereas no mice with the ez-146 MM1 showed the presence of metastases (Table I). The same results were obtained in mice injected with human tumor cells of different histology, such as untransfected and ez-146 HeLa cells (Table I). Mice transplanted with MM2 cells developed lymph node metastasis in 100% of the cases and lung metastasis in 81% of the cases. MM3 transplanted mice developed lymph node metastasis in 100% of the cases and lung metastasis in 78% of the cases. Again, ez-146 stable transfection abrogated metastasis formation.

Transfection of wild type ezrin resulted in lack of difference in incidence of local tumor and metastatic distribution, in respect to parental MM1–MM3 cells. The data obtained employing MM1–MM3 cells was statistically comparable, depicting that all 3 metastatic melanomas behaved in the same way in our *in vivo* human tumor xenograft model. After preliminary experiments for *in vitro* confirmation of *in vivo* results, we employed as a representative cell model MM1 in all the subsequent experiments.

This finding highlights a key role of ezrin in conferring a metastatic potential to human malignant melanoma cells, whereas it outlines the absence of a significant role of ezrin in the development of primary tumors.

Ezrin-related metastatic functions

Ezrin and tumor cell migration and invasion. The migratory capacity of tumors is one of the most important advantages of metastatic cells. To investigate the role of ezrin on tumor cell motility,

TABLE I – OVER-EXPRESSION OF ez-146 INHIBITS METASTASIS OF MELANOMA CELLS *IN VIVO* WITHOUT ALTERING PRIMARY TUMOR GROWTH

Cells inoculated	Incidence of local tumor (%)	Mean tumor weight (g)	Metastatic distribution/mice (%)		
			Lymph node	Lung	Liver
MM1	100	0.65 ± 0.08	100	80 ± 4	0
Ezrin-MM1	100	0.69 ± 0.08	100	80 ± 3	0
ez-146 MM1	100	0.68 ± 0.09	0	0	0
MM2	100	0.64 ± 0.04	100	81 ± 4	0
Ezrin-MM2	100	0.67 ± 0.04	100	80 ± 3	0
ez-146 MM2	100	0.64 ± 0.09	0	0	0
MM3	100	0.65 ± 0.04	100	78 ± 4	0
Ezrin-MM3	100	0.60 ± 0.1	100	80 ± 3	0
ez-146 MM3	100	0.67 ± 0.1	0	0	0
HeLa	100	0.71 ± 0.08	100	100	100
ez-146 HeLa	100	0.67 ± 0.09	0	0	0

Incidence of tumorigenicity, tumor weight at time of sacrifice and metastatic distribution of ez-146 MM1 and ezrin-GFP MM1 cells s.c. engrafted in SCID mice 45 days after tumor cell injection. In the last column incidence is expressed as percentage of mice bearing metastasis in the various organs. Each cell line was engrafted in 10 mice per experiment. The table is representative of one out of three experiments showing the mean values with their standard deviations.

we used a matrigel-free *in vitro* migration assay as described in materials and methods. Ez-146 MM1 displayed a marked reduction in their capacity to migrate through the filter membranes, in comparison to their untransfected counterpart (Fig. 1*b*). Similar results were obtained using HeLa cells (Fig. 1*b*). Ezrin deletion mutant induced a marked inhibition of migration also when transfected in MM2 and in MM3 (data not shown).

In order to confirm that the *in vivo* abrogation of metastatic dissemination induced by our ezrin deletion mutant was conserved in all its features also *in vitro*, we performed an invasion assay as detailed in materials and methods. Ez-146 transfected melanomas migration through matrigel was markedly decreased when compared with untransfected melanomas (Fig. 1*c*), once again highlighting that in the model analyzed, it targets a conserved mechanism.

One of the most important molecular actors of metastatic cell migratory activity is the adhesive transmembrane glycoprotein CD44,[42] whose interaction with ERM proteins is well known. We therefore analysed CD44-ezrin interaction in MM1 and ez-146 MM1. Previous data reported that CD44 and ezrin often possess different subcellular distribution.[43] Taking into consideration that the molecular interaction of a protein with pleiotropic functions such as ezrin could be difficult to reveal due to the rapidity to swift from 1 location to the other, we cross-linked the proteins before co-immunoprecipitation.[44] In MM1 and in HeLa cells (data not shown) CD44 and wild-type ezrin co-immunoprecipitated both in the absence and in the presence of ez-146 (Fig. 2). To highlight ez-146 molecular interactions in ez-146 MM1 which express both wild-type and the ezrin mutant, we employed ez-146 MM1 extracts, immunodepleted for wild-type ezrin, for co-immunoprecipitation experiments.[45] Interestingly, ez-146 continued to co-immunoprecipitated with CD44 also in the absence of wild type ezrin (Fig. 2). This data renders highly possible the hypothesis that the minimum N-terminal fragment of ezrin capable of having target activity in a cellular context was of 146 aminoacids. Previously, it has been demonstrated that aa 1–296 within the NERMAD is requested for head to tail interactions with wild type ezrin,[46] whereas to our knowledge no data was available on ezrin minimum fragment necessary to bind a membrane receptor. However, although ez-146 was able to interact with CD44, it did not bind with actin cytoskeleton. As far as wild-type ezrin-actin interactions are concerned, ezrin binds to actin also in the presence of the deletion mutant (Figs. 2*a* and 2*b*).

Previous reports have shown that binding between merlin and the CD44-Hyaluronic acid (HA) complex is a key mechanism in tumor suppressor activity of merlin.[47] Moreover, merlin overexpression inhibits CD44 mediated cell linkage to HA, in turn inhibiting the interaction of CD44 with both ezrin and actin.[48] We thus evaluated also merlin interaction with ezrin and CD44. The experiments showed that merlin co-immunoprecipitated with both

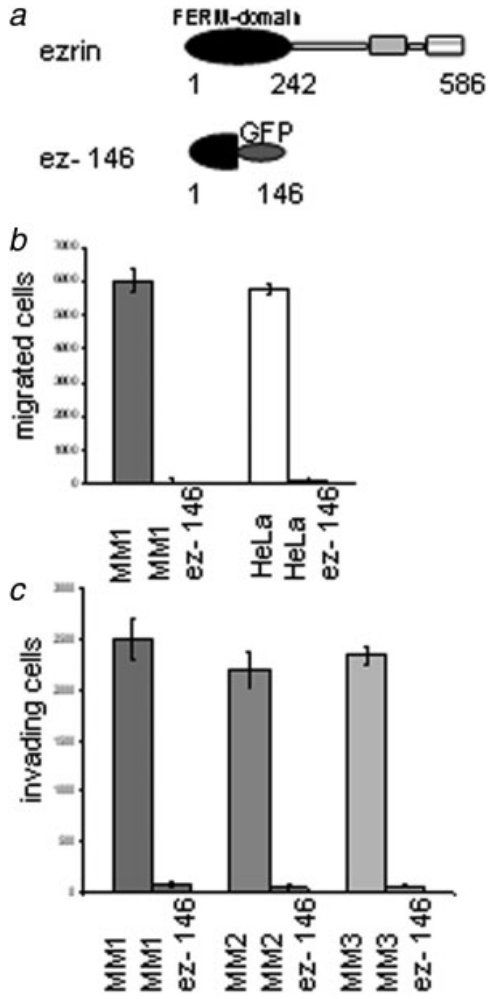

FIGURE 1 – Ezrin and ez-146 functional domains: over-expression of ez-146 inhibits metastatic melanoma cell migration. (*a*)The scheme represents wild-type and deletion mutant (ez-146) ezrin comprising of the following domains: FERM domain (black oval), α helical region (white bar), proline rich region (gray bar) and actin binding domain (striped bar), GFP (dark gray oval). Effects of ez-146 on cell migration and invasion *in vitro*. (*b*) MM1 and HeLa cells. Both untransfected and transfected counterpart for each cell type are shown. (*c*) Cells employed: metastatic melanomas (MM1, MM2 and MM3) Histograms are representative of 1 of 3 independent experiments. The cells are represented as follows: in different tones of gray the melanomas and in white HeLa cells.

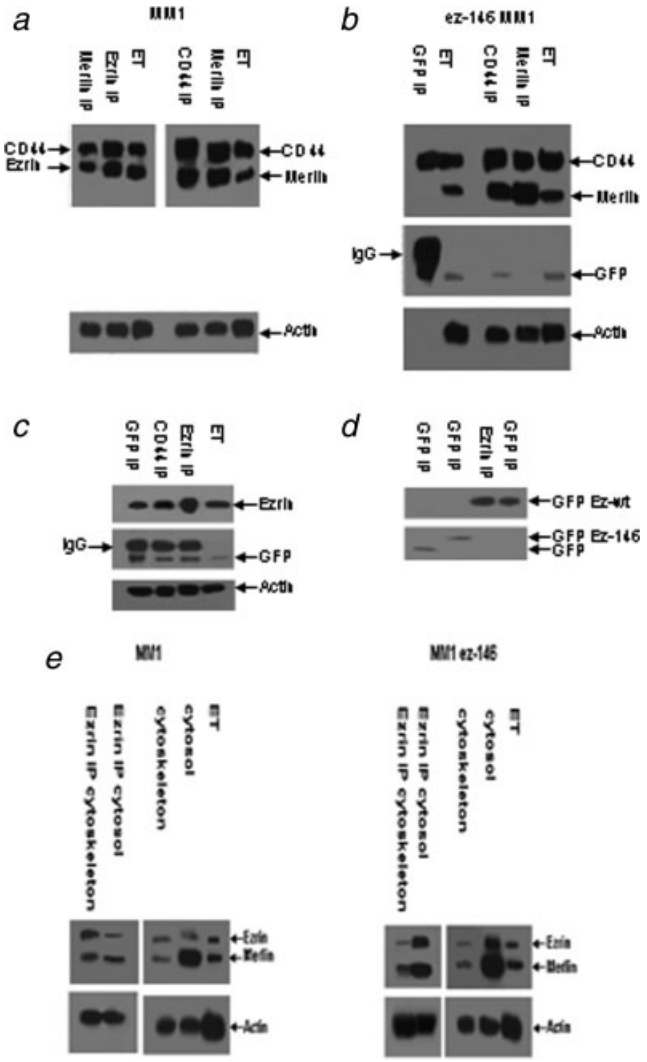

Figure 2 – Co-immunoprecipitation experiments of CD44/Merlin/Ezrin in MM1 and ez-146 MM1 cells. Western blot analysis of the expression of ezrin, ez-146, merlin and CD44 in 30 μg total cellular extract (ET) and 1-mg immunoprecipitates (IP) in (*a*) MM1 and in (*b–c*) MM1 ez-146, after both protein cross-linking and ezrin immunodepletion (the latter only for panel *b*). Panel *a*: right side immunoblotted with anti-CD44 and anti-merlin Abs. Left side: immunoblotted with anti-CD44 and anti-ezrin Abs. Panel *b*: immunoblotted with anti-CD44, merlin and GFP Abs as specified on the figure. Lower side of both panels: immunoblotted with anti-actin Ab to verify cytoskeletal integrity. Panel *c*: immunoblot of both wild-type and deletion mutant ezrin in MM1 ez-146 with anti-ezrin and anti-GFP Abs. Lower side of both panels: immunoblotted with anti-actin Ab to verify cytoskeletal integrity. Panel *d*: Anti-GFP immunoblot of MM1 transfected with empty GFP vector (lane 1), Ez-146 MM1 (lane 2) and Ez-GFP MM1 (3 and 4) cells. Panel *e*: immunoblotted with anti-Ezrin, Merlin and Actin. Cytosol and cytoskeleton cellular fractions were immunoprecipitated with anti-Ezrin. Panels *d* and *e* were obtained from cells that were not subjected to cross-linking or to immunodepletion.

ezrin and CD44 (Fig. 2*a*), but not with ez-146 (Fig. 2*b*), suggesting that when overexpressed this ezrin mutant competes with merlin for CD44 binding, shifting merlin interaction from this receptor to wild-type ezrin thus potentiating its tumor suppressor activity.[47,49] Moreover, these data suggest that the binding region of ezrin with merlin is included in the ezrin fragment downstream aminoacid 146.

Ezrin involvement in the phagocytic machinery of metastatic cells. Lamp-1 cellular distribution in MM1 and in ez-146 MM1

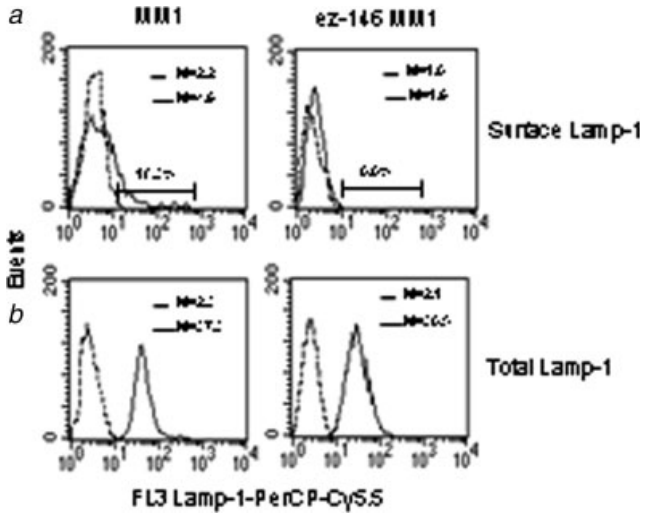

Figure 3 – Ezrin is involved in plasma membrane expression of the lysosomal antigen Lamp-1. Flow cytometry analysis of surface expression (*a*) and total amount (*b*) of Lamp-1 in a representative metastatic melanoma cell line (left panel) in comparison with the same cells transfected with ez-146 (right panel). Numbers in (*a*) represent the percentage of surface Lamp-1 positive cells; numbers in (*b*) represent the median values of fluorescence intensity histograms; dashed lines represent negative controls. One experiment representative of 3 is shown. Comparison between each set of values did not give statistically significant differences.

was evaluated by flow cytometry. Our results showed that plasma membrane Lamp-1 expression in MM1 was markedly higher in respect to ez-146 transfected cells. In fact, ez-146 expression induced a marked reduction of membrane Lamp-1 in comparison to untransfected MM1 cells. Importantly, total amount of Lamp-1 was not significantly different in the samples evaluated (Fig. 3). Further more, Western blot preliminary data depicted the absence of differences in Lamp-1 expression in MM1–MM3 cells total extracts (data not shown).

Analysis of a panel of 3 different metastatic melanoma cell lines revealed that plasma membrane surface expression of Lamp-1 was consistently similar. Transient transfection of metastatic cells with ez-146 dramatically decreased Lamp-1 plasma membrane expression, whereas total amount of Lamp-1 remained unaltered (Table II).

We then evaluated if differential Lamp-1 plasma membrane expression in metastatic melanomas depended on its connection to ezrin. Therefore, we analyzed ezrin and Lamp-1 association by immunofluorescence microscopy (Fig. 4). Lamp-1 and Ezrin co-localized in MM1, cells whereas in transfected MM1, Lamp-1 did not co-localize with ez-146.

To characterize in detail Lamp-1 and ezrin interactions, we used a fluorescence resonance energy transfer (FRET)-based approach in which the 2 molecules were respectively tagged with a donor (PE) and acceptor (Cy5) fluorophore. The statistical analysis of FRET efficiency (ET), calculated according to Riemann *et al.*[40] showed that in all MM cell lines considered (MM1–MM3) there was a significant association between Lamp-1 and ezrin (Fig. 5*a*).

Co-immunoprecipitation experiments further unraveled Lamp-1 and ezrin interaction dynamics because they enabled us to evaluate also ez-146 involvement, which due to the green fluorescence, could not be evaluated by FRET. In line with immunofluorescence results, Lamp-1 did not co-immunoprecipitate with ez-146, whereas in both MM1 and ez-146 MM1 cells Lamp-1 and ezrin co-immunoprecipitated (Figs. 5*b* and 5*c*). The same experiments demonstrated that the endosome marker Rab 5b behaved as Lamp-

TABLE II – Ez-146 EFFECT ON LAMP-1 PLASMA MEMBRANE EXPRESSION

Untransfected metastatic Melanoma cells	Surface Lamp-1 (%)	Total Lamp-1 (MFI)	Transfected metastatic melanoma cells	Surface Lamp-1(%)	Total Lamp-1 (MFI)
MM1	23.3 ± 4.1	28.8 ± 3.3	Ez-146 MM1	2.9 ± 1.3	40.3 ± 5.2
MM2	19.8 ± 3.2	37.7 ± 4.2	Ez-146 MM2	3.9 ± 2.1	39.8 ± 4.9
MM3	13.9 ± 4.9	47.6 ± 5.1	Ez-146 MM3	2.0 ± 0.5	35.6 ± 6.3

Flow cytometry analysis of surface and total expression of Lamp-1 in three metastatic melanomas (MM1-3) and their corresponding ez-146 transfected counterparts. Data reported are the mean ± standard deviation among four different experiments. Lamp-1 surface is expressed as percentage of cell surface Lamp-1 expressing cells. Total Lamp-1 is expressed as median values of fluorescence intensity (MFI).

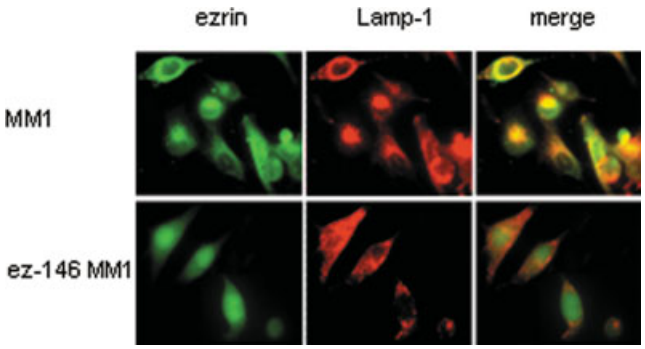

FIGURE 4 – Ezrin and Lamp-1 co-localization by immunofluorescence. Upper panel: MM1, lower panel: ez-146 MM1. Fluorescence labeling: left panel: wild-type ezrin (green fluorescence) in upper panel and in lower ez-146 GFP. Middle panel: Lamp-1 (red fluorescence). The upper right panel shows in yellow the regions of co-localization between ezrin (green) and Lamp-1 (red), whereas the lower right panel shows absence of ez-146 GFP/Lamp-1 co-localization.

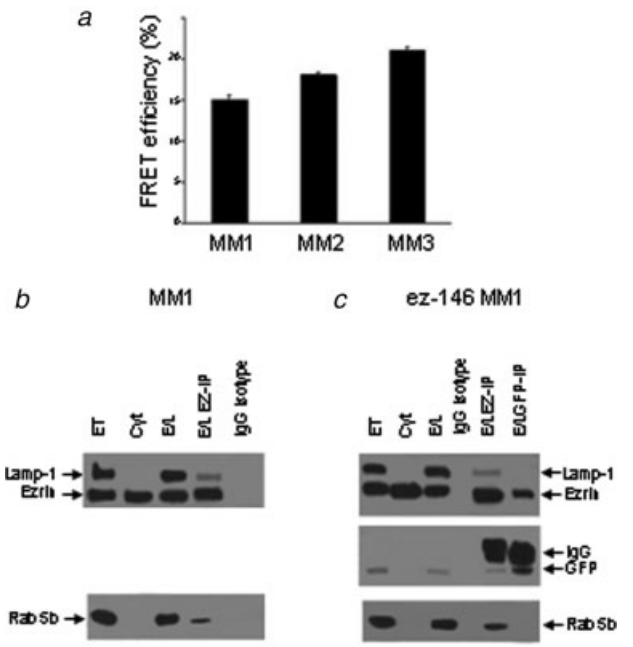

FIGURE 5 – Ezrin and Lamp-1 co-localization by FRET analysis and co-immunoprecipitation experiments. (*a*) FRET analysis of Ezrin and Lamp-1 interaction on 3 different metastatic melanoma cell lines. Results, reported as FRET efficiency, were obtained from 3 independent experiments and demonstrated a significant association between these 2 molecules. (*b*) and (*c*) Western blot analysis of Lamp-1, ezrin, ez-146, and Rab 5b protein expression in total cellular extracts (ET), endolysosomal compartment (E/L), cytosol (cyt); ezrin and ez-146 GFP immunoprecipitation (IP) of MM1 in (*b*) and in ez-146 MM1 in (*c*). Negative controls of IP were performed employing IgG isotypes. Lamp-1 is not detectable in EL ez-146 GFP immunoprecipitated (E/L GFP IP). The same is true for Rab 5b.

1 in connecting to wild type ezrin but not to ez-146 (Figs. 5*b* and 5*c*), supporting the hypothesis that ezrin is involved in vesicle trafficking of metastatic tumor cells.

Role of ezrin in acidification of metastatic cells intracellular vacuoles

We evaluated whether ez-146 induced abrogation of plasma membrane Lamp-1 expression might alter function of acidic vacuoles by analyzing differences in cellular uptake of the LysoTracker Red fluorescent dye in ez-146 MM1 and untransfected counterpart. We loaded both cell types with LysoTracker Red which can be used to visualize acidic late endocytic structures independent of endocytosis[50] and monitored both GFP and LysoTracker fluorescence. Possible blocks in downstream endocytosis, eventually induced by ez-146 transfection, would not induce variations of pH measurements in late endocytic structures when using LysoTracker Red. Moreover, the fluorophore conjugated to this probe, suited parallel detection with our fusion protein. To verify that the LysoTracker Red-labeled structures were indeed organelles with low pH, cells were treated with bafilomycin A1, a specific V-ATPase inhibitor.[51] MM1 were characterized by large acidic vacuoles, whereas ez-146 MM1 transfected cells displayed a marked reduction in LysoTracker Red accumulation. Moreover, bafilomycin A1 treatment drastically reduced LysoTracker Red accumulation, both in MM1 and in ez-146 MM1 transfected cells. Furthermore, bafilomicyn A1 effects on vesicle acidification was less pronounced in cells expressing deletion mutant ezrin as compared to untransfected cells (Fig. 6).

Discussion

Ezrin expression levels vary among melanoma types but existing data suggest that a significant overexpression is encountered in metastatic lesions with respect to primary tumors.[52,53] Here, we have shown that transfection of metastatic melanoma cells with N-terminal 146 aminoacids of ezrin, fused to GFP (ez-146) abrogated metastatic potential *in vivo*.

This was consistent with a reduction of *in vitro* migration, paralleled to ez-146 capacity of binding CD44 and lack of interaction with actin. Moreover, we show here for the first time, to our knowledge, that this N-terminal ezrin fragment of only 146 aminoacids can efficiently bind CD44. This result *per se* provides new information on molecular interaction between ezrin and CD44. On the other hand, we show that ezrin-merlin interaction involves the ezrin fragment downstream aminoacid 146. In fact, merlin while able to bind wild-type ezrin did not bind ez-146, as also supported by confocal microscopy analysis showing the absence of ez-146/merlin co-localization (not shown). This may also suggest that the abrogation of the metastatic phenotype due to ez-146 overexpression, could depend on unbound merlin capacity of exercising its tumor suppressor function (Figs 2*e* and 7). The molecular equilibrium between ezrin-CD44 and ezrin-merlin heterodimers is

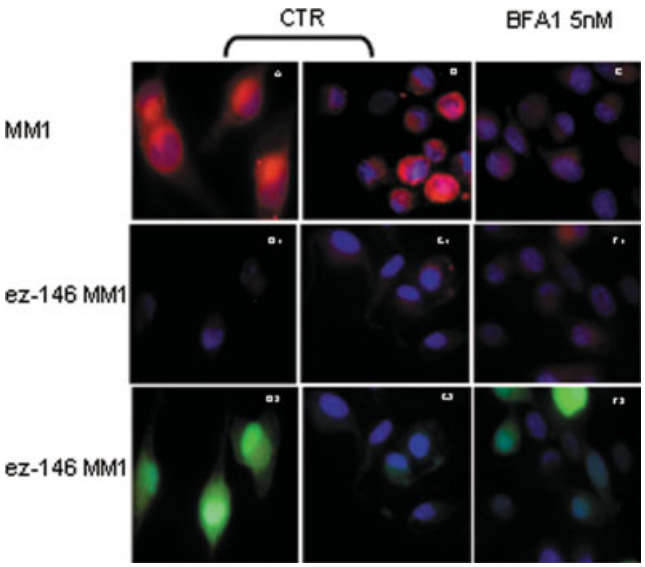

FIGURE 6 – Vacuolar acidity. LysoTracker Red labeled MM1 (upper pannel) and ez-146 MM1 (central and lower panel). Bafilomycin A1 treated cells (right column). Red fluorescence: upper and central panel (Lysotracker Red fluorescence). Green fluorescence: lower panel (GFP fluorescence). LysoTracker signal was observed in untreated MM1 (*a* and *b*) cells whereas in ez-146 MM1, it was markedly reduced (D_1 and E_1). Treatment of cells with Bafilomycin A_1 resulted in a significant degradation of the pH gradient (C and F_1) which confirmed the acidotrophic properties of LysoTracker Red. Left and central columns represent the same conditions as reported herein but at different enlargements.

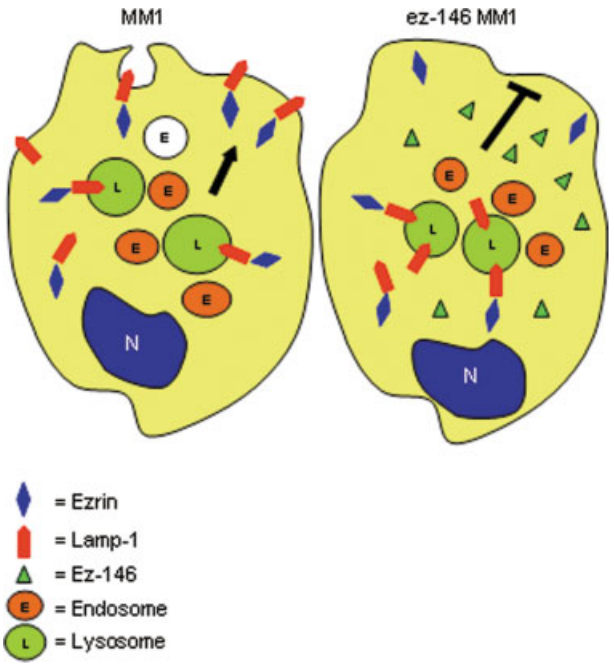

FIGURE 8 – Ez-146 possible role in impairment of Lamp-1 plasma membrane expression. Ez-146 might affect Lamp-1 cellular localization by impairing correct vesicular sorting.

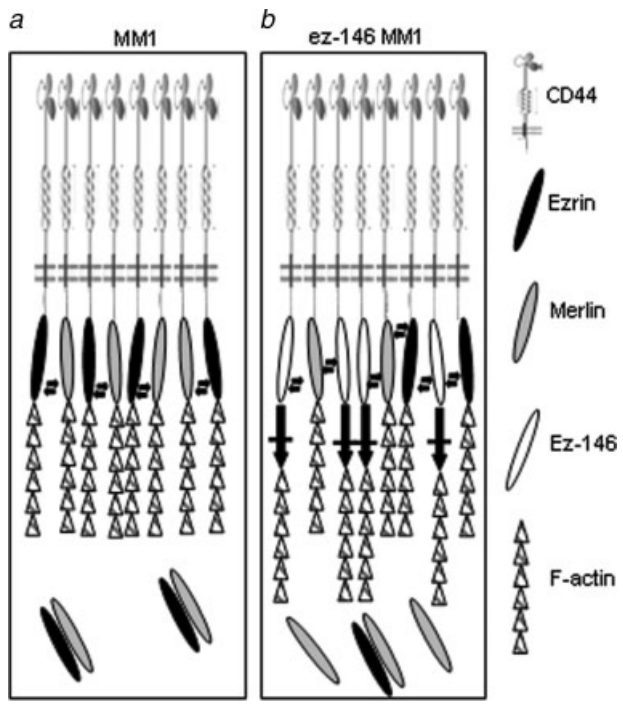

FIGURE 7 – Schematic representation of ezrin, ez-146, merlin and CD44 molecular interactions in (*a*) MM1 and (*b*) ez-146 transfected MM1. Ez-146 interaction with plasma membrane CD44 is likely to shift the molecular equilibrium of membrane merlin-CD44 and ezrin-CD44 towards cytosolic merlin-ezrin heterodymers or monomers, because it competes with such molecules for CD44 binding, without binding with them.

perturbed by the expression of ez-146 which suppresses a highly invasive and aggressive phenotype of the metastatic cells (Table II).

It is known that ezrin plays a specific role in modulating cannibal activity of metastatic tumor cells.[23,24] Our study shows that this function is specifically related to the connection between ezrin and some lysosomal (Lamp-1) and endosomal (Rab 5b) antigens, thus supporting a key role of ezrin in the cannibal machinery.[23] We show ezrin and Lamp-1 interaction in human melanoma through co-immunoprecipitation experiments, further supported by FRET analysis.[54]

Our data also reveal the existence of a clear relationship between plasma membrane localization of Lamp-1 and the metastatic phenotype of tumor cells. In fact, lack of Lamp-1 plasma membrane recruitment due to ez-146 transfection of metastatic melanomas, was consistent with both abolishment of *in vivo* metastatic behavior and marked reduction of phagocytic activity.

Recent data have suggested a possible involvement of Lamp-1 cell surface expression in the malignant progression of tumors.[34] In fact, Lamp-1 has been shown to mediate adhesion of tumor cells to vascular endothelial selectins, promoting or facilitating the metastatic process. It is also possible that Lamp-1 membrane expression may be involved in the increased invasive capacity of malignant melanoma cells, due to the presence of the cell surface of lysosomal-like structures that may facilitate nibbling of extracellular matrix components.

On the other hand we showed that ez-146 and Lamp-1 did not co-localize, thus not affecting the association of wild type ezrin with Lamp-1 in the endolysosomal compartment, but influencing Lamp-1 cellular distribution.

Our hypothesis (Fig. 8) is that over expression of ez-146 is not permissive to the proper plasma membrane localization of Lamp-1. It is likely that the ezrin fragment employed blocks vesicular trafficking to membrane because of lack of PIP_2 binding site on its C terminal region, maintaining nevertheless a vital phenotype

because of N terminal interactions with the plasma membrane through CD44.

This phenomenon correlated with impaired migratory and phagocytic activities of stably transfected ez-146 MM1 cells and was confirmed in a panel of transiently transfected metastatic melanoma (MM1–MM3) cells (Table II). We had previously reported that cannibalism of metastatic melanoma cells correlated with acidity of intracellular organelles as compared to cells deriving from primary tumors.[24] Therefore, we analyzed if the loss of metastatic potential induced by ez-146, was also correlated to a variation in the cellular acidic vacuolar compartment. In fact, we found that metastatic melanoma cells contained large acidic structures, whereas ez-146 transfected cells showed drastically reduced levels of acidic marker uptake. Moreover, the V-ATPase inhibitor bafilomycin A1 clearly inhibited LysoTracker Red uptake in melanoma cells, whereas mutant-ezrin transfected cells showed low LysoTracker Red uptake level also in the absence of bafilomycin A1 treatment. This clearly suggested that ezrin was directly involved in vacuole acidification. To note, vesicle acidification and trafficking is also involved in local invasion of metastatic cells, probably due to the activation of lytic enzymes participating to nibbling of the extracellular matrix.

Taken together, our results show that ezrin is widely involved in the exploitation of the metastatic process of human melanoma. Parallel work on metastatic phenomenon has been described by Sanchez-Madrid and colleagues, who highlighted tetraspanins involvement in colon carcinoma tumorigenic process, depicting once again how complex and cell type specific the events involved in human tumoral progression are.

We demonstrate that ezrin activity is mandatory for both the maintenance of migratory and invasive capacity of tumors and conservation of the ability to feed through other cells. This occurs through the specific molecular association between ezrin and molecules involved in many activities of metastatic cells, such as CD44 and Lamp-1. Particularly, the molecular interaction between ezrin and Lamp-1 was never been described together with its importance in allowing Lamp-1 membrane localization in metastatic cells. Here, we highlight that a molecular approach, through the use of ezrin deletion mutants, is highly effective in inhibiting metastatic behavior, through deregulation of the ezrin mediated linkage between actin and both CD44 and Lamp-1. The molecular consequence may pass also through the retrieval of the tumor suppressive activity of merlin.

References

1. Khanna C, Wan X, Bose S, Cassaday R, Olomu O, Mendoza A, Yeung C, Gorlick R, Hewitt SM Helman LJ. The membrane-cytoskeleton linker ezrin is necessary for osteosarcoma metastasis. Nat Med 2004;10:182–6.
2. Yu Y, Khan J, Khanna C, Helman L, Meltzer PS Merlino G. Expression profiling identifies the cytoskeletal organizer ezrin and the developmental homeoprotein Six-1 as key metastatic regulators. Nat Med 2004;10:175–81.
3. Mäkitie T, Carpén O, Vaheri A Kivelä T. Ezrin as a prognostic indicator and its relationship to tumor characteristics in uveal malignant melanoma. Invest Ophthal Vis Sci 2001;42:2442–9.
4. Akisawa N, Nishimorib I, Iwamurac T, Onishib S Hollingsworth MA. High levels of ezrin expressed by human pancreatic adenocarcinoma cell lines with high metastatic potential. Biochem Biophys Res Comm 1999;258:395–400.
5. Weng WH, Ahlén J, Aström K, Lui WO Larsson C. Prognostic impact of immunohistochemical expression of ezrin in highly malignant soft tissue sarcomas. Clin Cancer Res 2005;11:6198–204.
6. Slater M, Cooper M, Murphy CR. The cytoskeletal proteins alpha-actinin. Ezrin, and talin are De-expressed in endometriosis and endometrioid carcinoma compared with normal uterine epithelium. Appl Immunohistochem Mol Morpho 2007;15:170–4.
7. Chuan YC, Pang ST, Cedazo-Minguez A, Norstedt G, Pousette A Flores-Morales A. Androgen induction of prostate cancer cell invasion is mediated by ezrin. J Biol Chem 2006;281:29938–48.
8. Zhang Y, Hu MY, Wu WZ, Wang ZJ, Zhou K, Zha XL, Liu KD. The membrane-cytoskeleton organizer ezrin is necessary for hepatocellular carcinoma cell growth and invasiveness. J Cancer Res Clin Oncol 2006;132:685–97.
9. Geiger KD, Stoldt P, Schlote W Derouiche A. Ezrin immunoreactivity is associated with increasing malignancy of astrocytic tumors but is absent in oligodendrogliomas. Am J Pathol 2000;157:1785–93.
10. Bretscher A, Edwards K, Fehon RG. ERM proteins and merlin: integrators at the cell cortex. Nat Rev Mol Cell Bio 2002;3:586–99.
11. Helander TS, Carpén O, Turunen O, Kovanen PE, Vaheri A Timonen T. ICAM-2, redistributed by ezrin as a target for killer cells. Nature 1996;382:265–8.
12. Yonemura S, Hirao M, Doi Y, Takahashi N, Kondo T Tsukita S. Ezrin/radixin/moesin (ERM) proteins bind to a positively charged amino acid cluster in the juxta-membrane cytoplasmatic domain of CD 44. CD 43, and. ICAM-2. J Cell Biol 1998;140:885–95.
13. Gautreau A, Poullet P, Louvard D, Arpin M. Ezrin, a plasma membrane-microfilament linker, signals cell survival through the phosphatidylinositol 3-kinase/Akt pathway. Proc Natl Acad Sci USA 1999;96:7300–5.
14. Parlato S, Giammarioli AM, Logozzi M, Lozupone F, Matarrese P, Luciani F, Falchi M, Malorni W, Fais S. CD95 (APO-1/Fas) linkage to the actin cytoskeleton through ezrin in human T lymphocytes: a novel regulatory mechanism of the CD95 apoptotic pathway. EMBO J 2000;19:5123–34.
15. Lozupone F, Lugini L, Matarrese P, Luciani F, Federici C, Iessi E, Margutti P, Stassi G, Malorni W, Fais S. Identification and relevance of the CD95-binding domain in the N-terminal region of ezrin. J Biol Chem 2004;279:9199–207.
16. Luciani F, Matarrese P, Giammarioli AM, Lugini L, Lozupone F, Federici C, Iessi E, Malorni W, Fais S. CD95/phosphorylated ezrin association underlies HIV-1 GP120/IL-2-induced susceptibility to CD95(APO-1/Fas)-mediated apoptosis of human resting CD4(+)T lymphocytes. Cell Death Diff 2004;11:574–82.
17. Charrin S, Alcover A. Role of ERM (ezrin-radixin-moesin) proteins in T lymphocyte polarization, immune synapse formation and in T cell receptor-mediated signaling. Front Biosci 2006;11:1987–97.
18. Kishore R, Qin G, Luedemann C, Bord E, Hanley A, Silver M, Gavin M, Yoon YS, Goukassian D, Losordo DW. The cytoskeletal protein ezrin regulates EC proliferation and angiogenesis via TNF-alpha-induced transcriptional repression of cyclin A. J Clin Invest 2005;115:1785–96.
19. Underhill C. CD44: the hyaluronan receptor. J Cell Sci 1992;103:293–8.
20. Vaheri A, Carpén O, Heiska L, Helander TS, Jääskeläinen J, Majander-Nordenswan P, Sainio M, Timonen T, Turunen O. The ezrin protein family: membrane-cytoskeleton interactions and disease associations. Curr Cell Biol 1997;9:659–66.
21. Okada T, Lopez-Lago M, Giancotti FG. Merlin/NF-2 mediates contact inhibition of growth by suppressing recruitment of Rac to the plasma membrane. J Cell Biol 2005;171:361–71.
22. Sainio M, Jääskeläinen J, Pihlaja H, Carpén O. Mild familial neurofibromatosis 2 associates with expression of merlin with altered COOH terminus. Neurology 2000;54:1132–8.
23. Lugini L, Lozupone F, Matarrese P, Funaro C, Luciani F, Malorni W, Rivoltini L, Castelli C, Tinari A, Piris A, Parmiani G, Fais S. Potent phagocytic activity discriminates metastatic and primary human malignant melanomas: a key role of ezrin. Lab Invest 2003;83:1555–67.
24. Lugini L, Matarrese P, Tinari A, Lozupone F, Federici C, Iessi E, Gentile M, Luciani F, Parmiani G, Rivoltini L, Malorni W, et al. Cannibalism of live lymphocytes by human metastatic but not primary melanoma cells. Cancer Res 2006;66:3629–38.
25. Sarafian V, Jadot M, Foidart JM, Letesson JJ, Van den Brûle F, Castronovo V, Wattiaux R, Coninck SW. Expression of Lamp-1 and Lamp-2 and their interactions with galectin-3 in human tumor cells. Int J Cancer 1998;75:105–11.
26. Tomlinson J, Wang JL, Barsky SH, Lee MC, Bischoff J, Nguyen M. Human colon cancer cells express multiple glycoprotein ligands for E-selectin. Int J Oncol 2000;16:347–53.
27. Chen JW, Cha Y, Yuksel KU, Gracy RW, August JT. Isolation and sequencing of a cDNA clone encoding lysosomal membrane glycoprotein mouse LAMP-1. Sequence similarity to proteins bearing onco-differentiation antigens. J Biol Chem 1988;263:8754–8.
28. Fukuda M, Viitala J, Matteson J, Carlsson SR. Cloning of cDNAs encoding human lysosomal membrane glycoproteins, h-lamp-1 and h-lamp-2. Comparison of their deduced amino acid sequences. J Biol Chem 1988;263:18920–8.
29. Fukuda M. Lysosomal membrane glycoproteins. Structure, biosynthesis, and intracellular trafficking. J Biol Chem 1991;266:21327–30.
30. Youakim A, Romero PA, Yee K, Carlsson SR, Fukuda M, Herscovics A. Decrease in polylactosaminoglycans associated with lysosomal membrane glycoproteins during differentiation of CaCo-2 human colonic adenocarcinoma cells. Cancer Res 1989;49:6889–95.

31. Pierce M, Arango J. Rous sarcoma virus-transformed baby hamster kidney cells express higher levels of asparagine-linked tri- and tetraantennary glycopeptides containing [GlcNAc-beta (1,6)Man-alpha (1,6)Man] and poly-N-acetyllactosamine sequences than baby hamster kidney cells. J Biol Chem 1986;261:10772–7.
32. Kuźbicki L, Gajo B, Chwirot BW. Different expression of lysosome-associated membrane protein-1 in human melanomas and benign melanocytic lesions. Melanoma Res 2006;16:235–43.
33. Laferte S, Dennis JW. Purification of two glycoproteins expressing beta 1–6 branched Asp-linked oligosaccharides from metastatic tumor cells. Biochem J 1989;259:569–76.
34. Saitoh O, Wang WC, Lotan R, Fukuda M. Differential glycosylation and cell surface expression of lysosomal membrane glycoproteins in sublines of a human colon cancer exhibiting distinct metastatic potentials. J Biol Chem 1992;267:5700–11.
35. Arterburn LM, Earles BJ, August JT. The disulfide structure of mouse lysosome associated membrane protein 1. J Biol Chem 1990;265: 7419–23.
36. Sawada R, Lowe JB, Fukuda M. E-selectin-dependent adhesion efficiency of colonic carcinoma cells is increased by genetic manipulation of their cell surface lysosomal membrane glycoprotein-1 expression levels. J Biol Chem 1993;268:12675–81.
37. Rivoltini L, Kawakami Y, Sakaguchi K, Southwood S, Sette A, Robbins PF, Marincola FM, Salgaller ML, Yannelli JR, Appella E, Steven A. Rosenberg. Induction of tumor-reactive. CTL from peripheral blood and tumor-infiltrating lymphocytes of melanoma patients by in vitro stimulation with an immunodominant peptide of the human melanoma antigen. MART-1. J Immunol 1995;154:2257–65.
38. Lozupone F, Pende D, Burgio VL, Castelli C, Spada M, Venditti M, Luciani F, Lugini L, Federici C, Ramoni C, Rivoltini L, Parmiani G, et al. Effect of human natural killer and γδ cells on the growth of human autologous melanoma xenografts in SCID mice. Cancer Res 2004;64:378–85.
39. Gardella S, Andrei C, Ferrera D, Lotti LV, Torrisi MR, Bianchi ME, Rubartelli A. The nuclear protein HMGB1 is secreted by monocytes via a non-classical, vesicle-mediated secretory pathway. EMBO Rep 2002;3:995–1001.
40. Riemann DA, Tcherkes GH, Hansen J, Wulfaenger TB, Danielsen EM. Functional co-localization of monocytic aminopeptidase N/ CD13 with the Fc receptors CD32 and CD64. Biochem Biophys Res Commun 2005;331:1408–12.
41. Boya P, Andreau K, Poncet D, Zamzami N, Perfettini JL, Metivier D, Ojcius DM, Jäättelä M, Kroemer G. Lysosomal membrane permeabilization induces cell death in a mitochondrion-dependent fashion. J Exp Med 2003;197:1323–34.
42. Tsukita S, Oishi K, Sato N, Sagara J, Kawai A, Tsukita S. ERM family members as molecular linkers between the cell surface glycoprotein CD44 and actin-based cytoskeletons. J Cell Biol 1994;126:391–401.
43. Bretscher A, Reczek D, Berryman M. Ezrin: a protein requiring conformational activation to link microfilaments to the plasma membrane in the assembly of cell surface structures. J Cell Sci 1997;110:3011–8.
44. Green NS, Reisler E, Houk KN. Quantitative evaluation of the lengths of homobifunctional protein cross-linking reagents used as molecular rulers. Prot Sci 2001;10:1293–304.
45. Ajuh P, Kuster B, Joost K, Zomerdijk CBM, Mann M, Lamond AI. Functional analysis of the human CDC5L complex and identification of its components by mass spectrometry. EMBO J 2000;19:6569–81.
46. Gary R, Bretscher A. Ezrin self-association involves binding of an N-terminal domain to a normally masked C-terminal domain that includes the F-actin binding site. Mol Biol Cell 1995;6:1061–75.
47. McClatchey AI. Merlin and ERM proteins: unappreciated roles in cancer development? Nat Rev Cancer 2003;3:877–83.
48. Bai Y, Liu YJ, Wang H, Xu Y, Stamenkovic I, Yu Q. Inhibition of the hyaluronan-CD44 interaction by merlin contributes to the tumor-suppressor activity of merlin. Oncogene 2007;26:836–50.
49. Sun CX, Robb VA, Gutmann DH. Protein 4.1 tumor suppressors: getting a FERM grip on growth regulation. J Cell Sci 2002;115:3991–4000.
50. Bucci C, Thomsen P, Nicoziani P, McCarthy J, van Deurs B. Rab7: a key to lysosome biogenesis. Mol Biol Cell 2000;11:467–80.
51. Bowman EJ, Bowman BJ. Purification of vacuolar membranes, mitochondria, and plasma membranes from *Neurospora crassa* and modes of discriminating among the different H+-ATPases. Methods Enzymol 1988;157:562–73.
52. Ilmonen S, Vaheri A, Asko-Seljavaara S, Carpén O. Ezrin in primary cutaneous melanoma. Modern Pathol 2005;18:503–10.
53. Moilanen J, Lassus H, Leminen A, Vaheri A, Bützow R, Carpén O. Ezrin immunoreactivity in relation to survival in serous ovarian carcinoma patients. Gynecol oncol 2003;90:273–81.
54. Stryer L. Fluorescence energy transfer as a spectroscopic ruler. Annu Rev Biochem 1978;47:819–46.